Available online at www.sciencedirect.com
ScienceDirect
Catalysis Today 131 (2008) 533–540
CATALYSIS TODAY
www.elsevier.com/locate/cattod

CH_4/CO_2 reforming over La_2NiO_4 and 10%NiO/CeO_2–La_2O_3 catalysts under the condition of supersonic jet expansion via cavity ring-down spectroscopic analysis

L. Li [a], B.S. Liu [a,b,*], J.W.H. Leung [a], C.T. Au [c], A.S.-C. Cheung [a,**]

[a] Department of Chemistry, The University of Hong Kong, Pokfulam Road, Hong Kong, China
[b] Department of Chemistry, Tianjin University, Tianjin 300072, China
[c] Department of Chemistry and Centre for Surface Analysis and Research, Hong Kong Baptist University, Kowloon Tong, Hong Kong, China

Available online 26 November 2007

Abstract

CH_4/CO_2 reforming over La_2NiO_4 and 10%NiO/CeO_2–La_2O_3 catalysts under the condition of supersonic jet expansion was studied via direct monitoring of the reactants and products using the sensitive technique of cavity ring-down spectroscopy. Vibration–rotational absorption lines of CH_4, H_2O, CO_2 and CO molecules were recorded in the near infrared spectral region. Our results indicated that La_2NiO_4 is superior to 10%NiO/CeO_2–La_2O_3 in performance. In addition, we observed enhanced reverse-water-gas-shift reaction at augmented reaction temperature. The formation of reaction intermediates was also investigated by means of time-of-flight mass spectrometry and there was the detection of CH_x^+, OH^+ and H^+ species.

Keywords: CH_4/CO_2 reforming; Supersonic jet expansion; Cavity ring-down spectroscopy; Vibration–rotational spectra; Carbon deposition; TOF-MS

1. Introduction

In the last two decades, CO_2 reforming of methane has attracted much attention due to both commercial and environmental reasons. One advantage of dry reforming is that compared to the approaches of steam reforming and partial oxidation, CO_2 reforming of methane would result in lower H_2:CO ratio which is preferred in the synthesis of oxygenated compounds [1,2]. Furthermore, CO_2 is a cheap and clean source of oxygen, and the adoption of it as oxidant would avoid the O_2 separation plants needed for CH_4/O_2 partial oxidation. The other advantage of CH_4/CO_2 reforming was the availability of CH_4 and CO_2 at low or even negative prices [3]. Natural gas contains primarily CH_4 and it is known that there could be CO_2 in large fractions [4–6]. Many sources of natural gas are located in remote regions and the methane presence might not be high enough for any commercial purposes. It is well known that there is inevitable release and burning of methane. With the worsening of global warming, a proper utilization of CH_4 and CO_2 would be a double bonus. The major obstacle for commercialization of the CH_4/CO_2 reforming process is the rapid deactivation of catalysts induced by carbon deposition. In our previous studies [7–11], improved stability in CH_4/CO_2 reforming at the temperatures of around 700 °C was observed over a series of La_2NiO_4 catalysts. Nevertheless, the catalysts deactivate ultimately after prolong operation at high temperatures. It has been disclosed that CeO_2 is an effective promoter and/or support for Ni-based catalysts. In general, with the addition of ceria, there is an improvement in dispersion of nickel particles and enhancement in resistance towards carbon deposition in CH_4/CO_2 reformation [12–14]. In this study, we compared the catalytic performance of La_2NiO_4 and 10%NiO/CeO_2–La_2O_3 catalysts for the purpose of understanding the mechanistic aspects of ceria.

In recent exploratory investigations, it was observed that when CH_4/CO_2 reforming was allowed to occur at a short time scale of ca. 10^{-3} s, the products are drastically different from those observed under the usual equilibrium conditions [15–17]. Such a short reaction time can be easily achieved by expanding a reactant gas through a 0.1-mm nozzle either containing or

* Corresponding author at: Department of Chemistry, Tianjin University, Tianjin 300072, China.
** Corresponding author: Department of Chemistry, The University of Hong Kong, Pokfulam Road, Hong Kong.
E-mail addresses: bingsiliu@tju.edu.cn (B.S. Liu), hrsccsc@hku.hk (A.S.C. Cheung).

0920-5861/$ – see front matter
doi:10.1016/j.cattod.2007.10.087

made of catalytic materials. The strong flow and the imposed short contact time fosters rapid desorption of intermediates into the gas phase, thereby restricting interaction of reactive intermediates and/or products with the surface of the catalyst. The detection of intermediates and products is made possible downstream in a collision-free supersonic beam environment.

In this work the CH_4/CO_2 reforming reaction was investigated under the condition of supersonic jet expansion and the products were directly analyzed by time-of-flight mass spectrometer (TOF-MS) and cavity ring-down spectroscopy (CRDS). The combination of a supersonic free jet and the fast CRDS monitoring technique allows the study of catalytic reactions *in situ*. The supersonic jet arrangement limits the contact and interaction time between the catalyst and reactants, and the fast CRDS allows the detection and monitoring of reactants, intermediate species and/or products. Comparing with the commonly used *in situ* FT-IR spectroscopic technique, CRDS has much higher sensitivity because of the multiple passes arrangement [18]. This advantage is important particularly for detecting molecular species at low concentration. In the course of investigation, we monitored the molecular transition lines of water molecules to track the progress of the reverse-water-gas-shift (RWGS, i.e. $CO_2 + H_2 = CO + H_2O$) reaction. Two catalysts, viz. La_2NiO_4 and $10\%NiO/CeO_2–La_2O_3$ were examined before and after the CH_4/CO_2 reforming reaction and were characterized by means of temperature-programmed reduction (TPR) and high-resolution transmission electron microscopy (HRTEM).

2. Experimental

2.1. Preparation of $LaNiO_4$ and $10\%NiO/CeO_2–La_2O_3$ catalysts

The $LaNiO_4$ precursor was synthesized by means of a sol–gel method reported elsewhere [19]. To put it briefly, stoichiometric $Ni(NO_3)_2{\cdot}6H_2O$ and La_2O_3 were dissolved in a small amount of diluted nitric acid, and citric acid and ethylene glycol were added to it; the molar amount of citric acid was 1.5 times that of total metal ions. Then, the solution was heated to 60 °C with constant stirring. After water removal via evaporation, a translucent green gel was obtained which was subsequently aged and dried at room temperature (RT) for 3 days, followed by calcination at 500 °C for 4 h. The as-generated catalyst is denoted as "La_2NiO_4" hereinafter. For comparison, a $10\%NiO/CeO_2–La_2O_3$ catalyst was prepared in a similar manner with the employment of 3.1084 g $Ni(NO_3)_2{\cdot}6H_2O$, 14.1380 g $Ce(NO_3)_3{\cdot}6H_2O$ and 1.6083 g La_2O_3.

2.2. CRDS analysis in supersonic jet expansion

A schematic diagram of the experimental setup is shown in Fig. 1. It consists of a tunable pulsed dye laser system with a Raman shift tube, a ring-down cavity, a heater assembly, a photodiode detector and a computer system for retrieving absorption signals. The setup for performing CRDS has been described elsewhere [20–22], and only a brief description of the relevant experimental conditions and the use of the Raman shift tube for generating near infrared radiation are given here. Catalytic reaction of CO_2 reforming of CH_4 was carried out at a fixed-bed quartz reactor with an inner diameter of 4 mm. The catalyst (50 mg) was secured between two quartz-wool plugs in the reactor, and a thermocouple placed underneath the quartz reactor at the center of the catalyst bed was deployed for the control of reaction temperature. The feeding of reactant mixture was regulated by means of an electronic pulsed valve. The chemical composition of the effluent exited from the quartz reactor was monitored by means of the CRDS and TOF-MS [17] techniques. A Nd:YAG (Spectra Physics Lab-170, 400 mJ/pulse at 532 nm) pumped-dye laser (Sirah PRSC-D) system operating at 10 Hz was used to generate tunable laser pulses in the 610–650 nm region using the DCM and the 670–720 nm region using the LDS dye. The output of the dye laser was

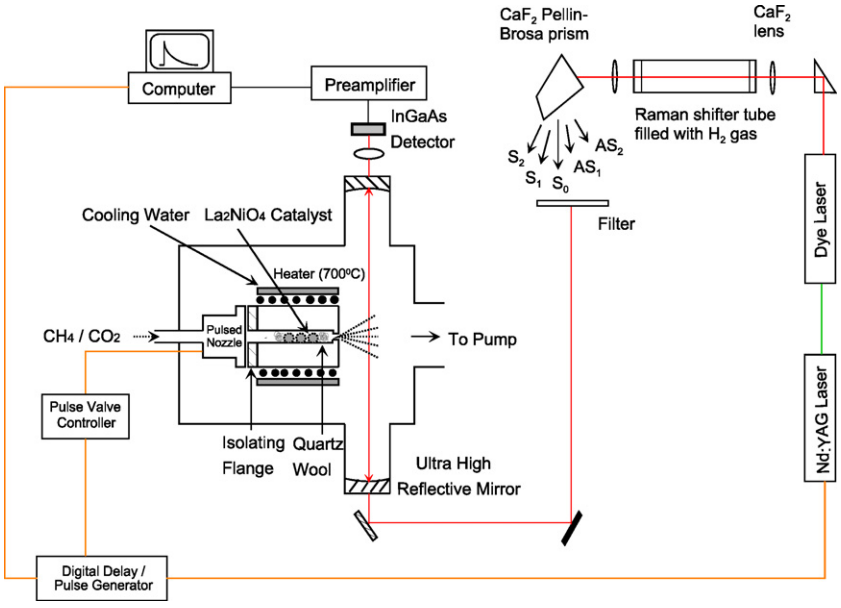

Fig. 1. Schematic diagram of the CRDS apparatus.

focused by a CaF_2 lens ($f = 50$ cm) and entered a 1-m long home-built Raman shift tube filled with ca. 120 psi of hydrogen gas for frequency shifting the dye laser radiation to longer wavelength region. After passing through the shift tube, laser radiation was dispersed by a CaF_2 Pellin–Broca prism and filtered by a 1.0 μm long pass filter (Thorlabs FGL 1000S) to eliminate the anti-Stokes and first-order Stokes lines. Laser radiation with power about 1 mJ and wavelength around 1.2–1.6 μm (the second Stokes line) was eventually delivered to the ring-down cavity. An InGaAs (Thorlabs PDA 400) photodiode was used to detect the laser radiation exited from the end mirror. The electronic signal from the detector was amplified and averaged. Data acquisition and cavity ring-down data processing were performed by a computer system using Labview software.

2.3. Characterization of catalysts

TPR of La_2NiO_4 and 10%NiO/CeO_2–La_2O_3 catalysts was carried out in a quartz tube reactor with an 8 mm inner diameter using a 5%H_2/Ar mixture for reduction. The sample (100 mg) was loaded in the middle part of the reactor, and a liquid-nitrogen trap was placed at the outlet for the removal of water. The temperature was ramped from 50 °C to 900 °C at a rate of 10 °C/min and kept at 900 °C for 5 min. The amount of consumed hydrogen was measured by means of a thermal conductivity detector (TCD) and an on-line computer was used for data acquisition and analysis.

The morphology and selected area electron diffraction (SAED) pattern of catalysts and deposited carbon were observed using a HRTEM (Tecnai G2 F20) instrument (also equipped for energy dispersive X-ray (EDX) analysis). The procedure for sample preparation and operating parameters for the analysis are similar to those reported in Ref. [23].

3. Results and discussion

3.1. Physical properties of La_2NiO_4 and 10%NiO/CeO_2–La_2O_3

The TPR profiles of La_2NiO_4 and 10%NiO/CeO_2–La_2O_3 catalysts are shown in Fig. 2. In the case of La_2NiO_4, beside a shoulder peak at ca. 353.8 °C, there were two big H_2-reduction peaks at 250 °C and 642.4 °C. As disclosed [19], for the reduction of NiO there is a shoulder and a big reduction peak at 350 °C and 400 °C, respectively. We hence assign the peaks at 250 °C and 353.8 °C to reduction of highly dispersed NiO species whereas the big peak at 642.4 °C to the reduction of La_2NiO_4. As for the 10%NiO/CeO_2–La_2O_3 catalyst, beside the very small peak at 443 °C, there is the dominant one at 288.6 °C, implying that the NiO component was uniformly dispersed on the surface of the CeO_2/La_2O_3 support. The HRTEM images of the as-prepared sample (Fig. 3) revealed that unlike La_2NiO_4 which is ball-like [22], 10%NiO/CeO_2–La_2O_3 displayed morphology of irregular structure. The diffuse rings of SAED pattern taken from local region of the catalyst (inset of Fig. 3) suggest the presence of polycrystalline nickel

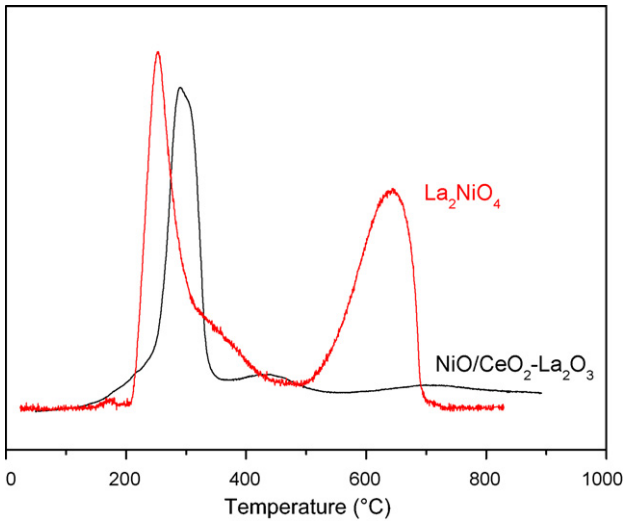

Fig. 2. TPR profiles of La_2NiO_4 and 10%NiO/CeO_2–La_2O_3.

particles of small size. In other words, there is no generation of new nickel compounds during the preparation of 10%NiO/CeO_2–La_2O_3, and interaction between NiO and CeO_2–La_2O_3 is weak.

3.2. TOF-MS analysis

Fig. 4 shows the mass spectra of species produced over 10%NiO/CeO_2–La_2O_3 under supersonic jet expansion condition with a variation in reactant feed. In the initial stage of CH_4 exposure, methane reacted with the oxygen of 10%NiO/CeO_2–

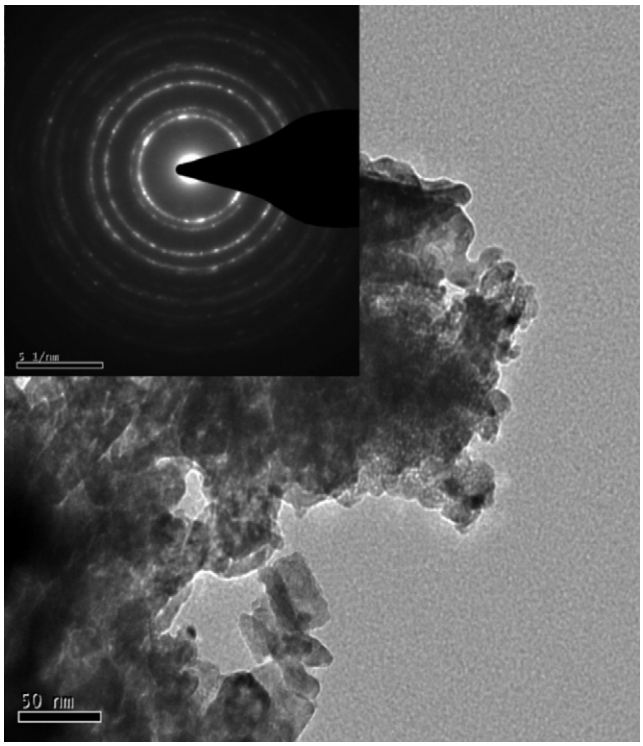

Fig. 3. Fine structure and SAED pattern (inset) of as-prepared 10%NiO/CeO_2–La_2O_3.

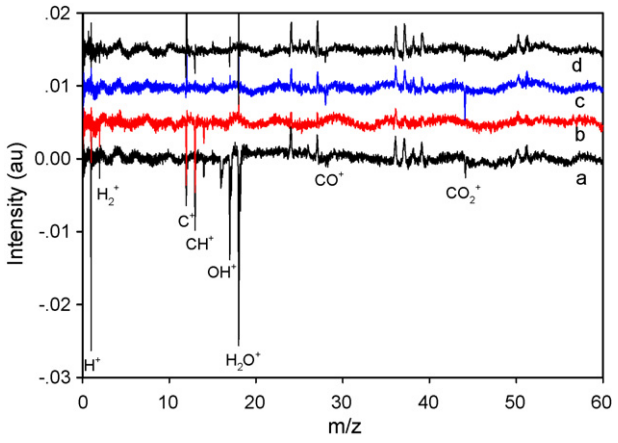

Fig. 4. TOF-MS signals of products over 10%NiO/CeO_2–La_2O_3 at 620 °C: (a) exposure to CH_4 for 5 min, (b) exposure to CH_4 for 30 min, (c) exposure to CO_2 for 5 min and (d) exposure to CH_4/CO_2(1:1) for 5 min (pulsing rate was 0.33 ms/10 Hz).

La_2O_3 according to the following equations:

$$CH_4 + NiO/CeO_2{-}La_2O_3 = Ni^0 + CeO_2{-}La_2O_3 + CH_x + OH + (3-x)\,H \quad (3.2a)$$

$$OH + H = H_2O \quad (3.2b)$$

$$CH + OH = CO + H_2 \quad (3.2c)$$

$$CO + O* = CO_2 \quad (3.2d)$$

$$CH_x = C + xH \quad (3.2e)$$

$$2H = H_2 \quad (3.2f)$$

We observed copious amount of H_2O^+, OH^+, CO^+, $CO_2{}^+$, H^+ and C^+ (Fig. 4a); with time on-stream, the signals of CO_2, CO and H_2O declined gradually to disappearance whereas there was a remarkable rise in the signals of H^+ and CH_x (x = 0, 1, 2, 3) (Fig. 4b), a clear indication of CH_4 decomposition on the Ni^0 active sites. If the feed was switched from CH_4 to CO_2, there was significant reduction in signal of CH_x (x = 0, 1, 2, 3), suggesting that the surface species interacted with CO_2 to form CO via the CHO intermediate (i.e. $CO_2 + CH_x = CHO + CH_{x-1}O$) [22] (Fig. 4c). If CH_4 and CO_2 (1:1 molar ratio) were co-fed into the reactor, strong signals of CH_x, H_2O, CO, CO_2 and H_2 were observed (Fig. 4d). The results indicated that CH_4/CO_2 reforming and RWGS reaction occurred simultaneously under the condition of supersonic jet expansion. In addition, due to the fast departure of species from the surface of the catalyst, the $CH_x{}^+$, OH^+ and H^+ intermediates were detected. In this case, the species detected by the TOF-MS technique can be related to a multi-photon ionization of CH_4, CO_2 and H_2O.

3.3. CRDS analysis

For the monitoring of reactants consumption and the products formation, we collected high-resolution absorption spectra of vibration–rotational transitions of CH_4, H_2O, CO_2 and CO molecules in the near infrared spectral region. The selection of the near infrared rather than the mid infrared region is because congestion of molecular transition lines in the former is relatively less, and more than one molecule can be examined simultaneously in certain ranges. The CRDS spectra of CH_4 and H_2O were observed in the 7480–7505 cm^{-1} (1.33 μm) range, whereas those of CO_2 and CO in the 6360–6370 cm^{-1} (1.57 μm) range. In this paper, we follow the systematic scheme for numbering normal modes of vibration and labeling of vibrational states in polyatomic molecules as stated by Hollas [24]. The details of the vibration–rotational transitions are listed in Table 1.

Besides the stable reactants and products, unstable intermediates such as CH_x (x = 1, 2, 3) were also monitored during CH_4/CO_2 reforming over the 10%NiO/CeO_2–La_2O_3 and La_2NiO_4 catalysts. Fig. 5 shows the cavity ring-down absorption signals of CH_4 consumption and water formation over La_2NiO_4 at different temperatures. The results revealed that with the increase of reaction temperature, CH_4 conversion increased gradually accompanied with the occurrence of RWGS reaction. According to McIlroy [29], CH_2 spectrum fragment of the (0,13,0)–(0,0,0) band at 622.2–622.8 nm was observed over a CH_4/O_2/Ar flame. In principle, CH_4 decomposition over La_2NiO_4 should accompany with the formation of CH_x (x = 1, 2, 3) intermediates. However, we detected no signal of $^1CH_2$ in CH_4/CO_2 reforming or in direct CH_4 decomposition over La_2NiO_4. The results suggested that the CH_x intermediates existed as adsorbed species on the surface of catalyst and their presence in the gas-phase was too low to be detected by the CRDS technique.

Shown in Fig. 6(i) and (ii) are the CRDS signals of CO_2 consumption and CO formation recorded over La_2NiO_4 and 10%NiO/CeO_2–La_2O_3, respectively, in the temperature range of 400–750 °C. The variation of CO_2 and CO bands indicated that CO_2 consumption and CO formation increased with temperature rise. At 600 °C over La_2NiO_4, there was almost no detection of CO_2 but CO_2 signal was still observed over 10%NiO/CeO_2–La_2O_3. The results disclosed clearly that La_2NiO_4 was superior to 10%NiO/CeO_2–La_2O_3 in converting CO_2, in concord with the exposition based on the spinal

Table 1
Vibration–rotational absorption lines in the near infrared spectral region as detected in CRDS analysis

Molecule	Point group symmetry	Spectral region (cm^{-1})	Vibrational transition	Rotational transition	References
CH_4	T_d	7480–7500	$2_0^1 3_0^2$	$\Delta J = 0$ (Q branch)	[25]
H_2O	C_{2v}	7485.1	$1_0^1 3_0^1$	$6_{3,3}$–$5_{1,4}$	[26]
CO_2	$D_{\infty h}$	6357–6370	$1_0^3 2_0^{0,0} 3_0^1$	R(12)–R(34)	[27]
CO	$C_{\infty h}$	6357–6368	3–0	R(1)–R(4)	[28]

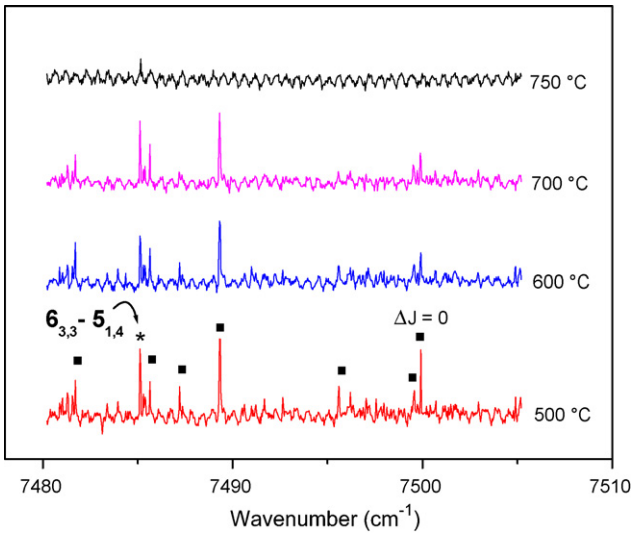

Fig. 5. CRDS signal of CH_4 consumption (■) and H_2O formation (✱) recorded over La_2NiO_4 at different temperatures.

structure of La_2NiO_4 [22]. Furthermore, at 700 °C only absorption signals of CO were observed over both catalysts, indicating that CH_4/CO_2 reforming was favorably run under the condition of supersonic jet expansion.

If one wanted to further study the RWGS reaction a real time control of changing, for instance, the composition of the reactants could be imposed, and the effects of such change would be immediately known. In addition, in our experiments the CRDS signal was obtained by scanning the tunable laser; in fact, the laser output can be tuned to a particular wavelength for monitoring the absorption signal of a particular molecular species. The shortest time for obtaining a single CRDS signal is 10^{-6} s, which should be good enough for detecting even short life-time intermediate species. The CRDS technique involves the use of a very high finesse optical cavity and such cavity has an intrinsic disadvantage of having a small dynamic range for the measurement of concentration of the molecular species. However, this disadvantage could be overcome by careful selection of molecular transition lines with appropriate absorption cross-section. When the species to be measured inside the cavity is of low concentration, a large cross-section absorption molecular line should be used and vice versa.

3.4. Stability of catalysts and formation of coke

Fig. 7(i) and (ii) shows the CRDS spectra of, respectively, CO and CO_2, and CH_4 and H_2O recorded over La_2NiO_4 in CH_4/CO_2 reforming at 700 °C and different on-stream times. Fig. 8(i) and (ii) shows similar spectra but were recorded over the 10%NiO/CeO_2–La_2O_3 catalyst. The intensity of CH_4 and CO_2 signals increased gradually with time, indicating that deactivation of the catalysts occurred only at a much later stage. In order to compare the stability of the two catalysts, the conversion of CO_2 and CH_4 over 10%NiO/CeO_2–La_2O_3 and La_2NiO_4 was estimated by an integration of CRDS peak areas. The results disclosed that the initial conversion of CH_4 and CO_2, respectively over La_2NiO_4 in supersonic jet expansion

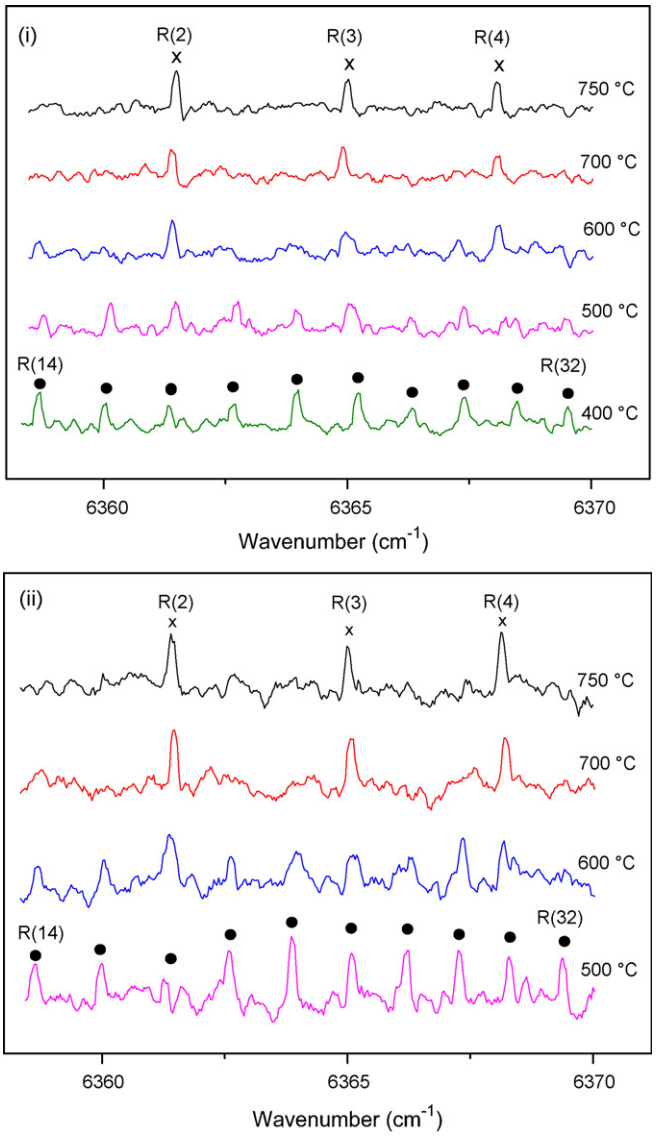

Fig. 6. CRDS signals of CO_2 consumption (●) and CO formation (×) recorded over (i) La_2NiO_4 and (ii) 10%NiO/CeO_2–La_2O_3, respectively, at different temperatures.

was 68% and 82%, and over 10%NiO/CeO_2–La_2O_3 was 48% and 75%, which is higher than those (ca. 58% and 71% over La_2NiO_4 [19], and 33.5% and 50.3% over10%NiO/CeO_2–La_2O_3 [inset of Fig. 9], respectively) observed under traditional condition of one atmospheric pressure. It has been reported by Wang and Lu [30] that during long period of methane reforming, the acidic property as well as the oxygen storage and/or the oxygen release/adsorption ability of CeO_2 favor the oxydehydrogenation of methane. We observed that after on-stream time of 6 h, CH_4 conversion over 10%NiO/CeO_2–La_2O_3 became slightly higher than that over La_2NiO_4, plausibly due to the unique natures of the CeO_2 additive. As observed from the CRDS spectra of CH_4 and H_2O, the signal intensity of H_2O (Figs. 7(ii) and 8(ii)) increased with time on-stream. This could be a result of the RWGS reaction being favorable under the condition of supersonic jet expansion. The fact that the conversion of CO_2 was remarkably higher than that of CH_4

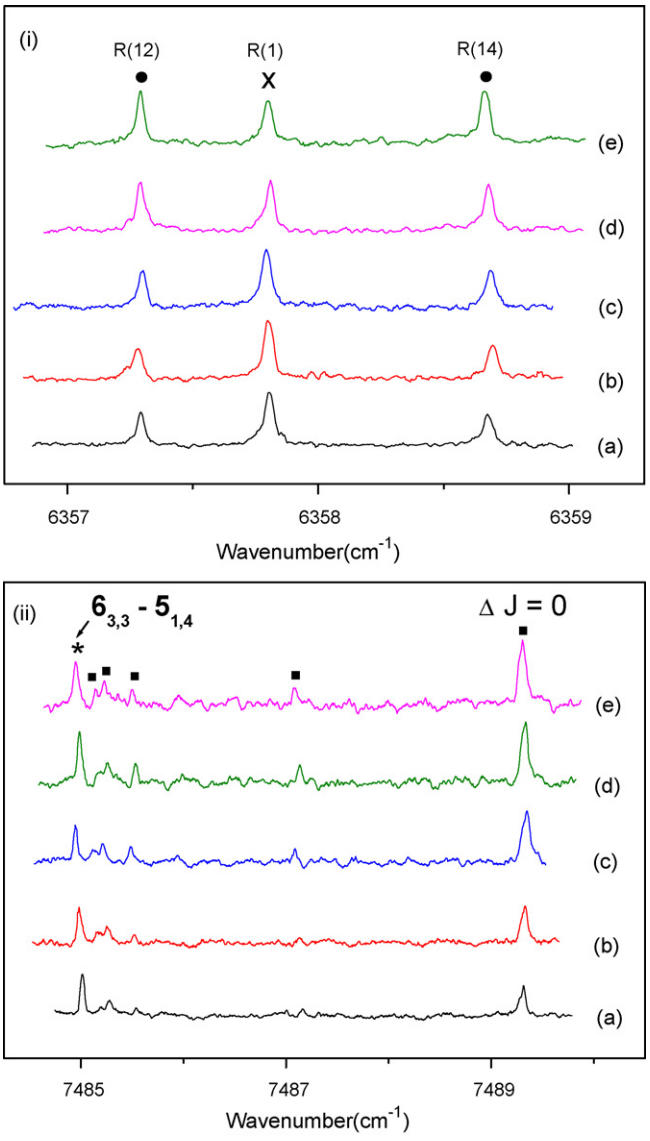

Fig. 7. CRDS spectra of (i) CO (×) and CO_2 (●), (ii) CH_4 (■) and H_2O (✱) over La_2NiO_4 catalyst in CH_4/CO_2 reforming at 700 °C recorded at (a) 0 h, (b) 4 h, (c) 8 h, (d) 12 h and (e) 16 h on-stream time.

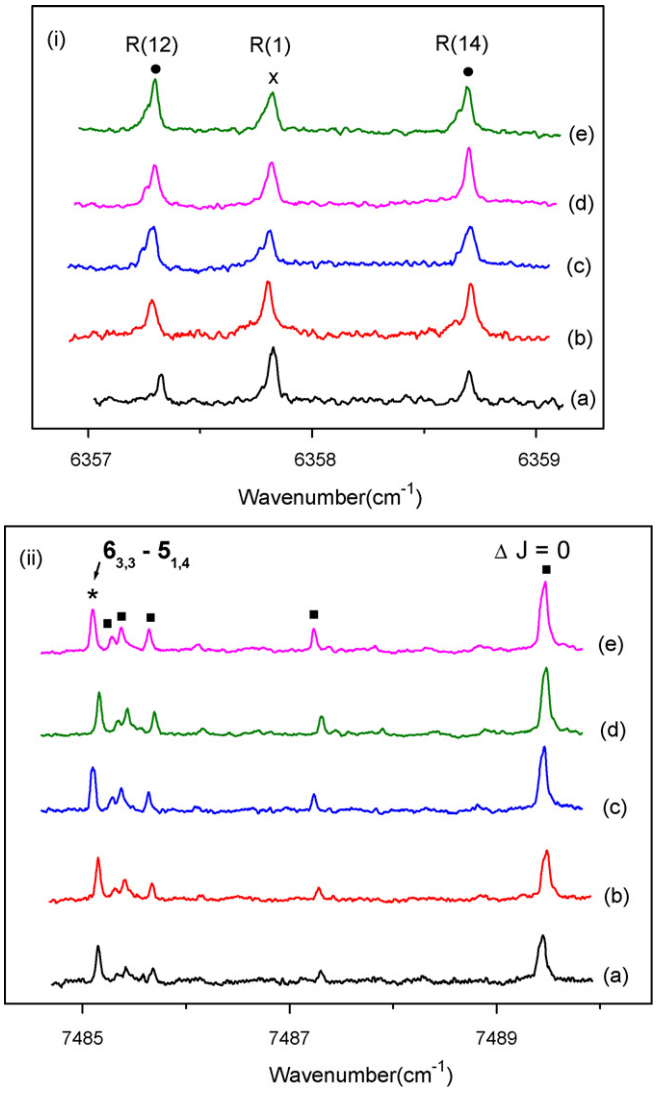

Fig. 8. CRDS spectra of (i) CO (×) and CO_2 (●), (ii) CH_4 (■) and H_2O (✱) over 10%NiO/CeO_2–La_2O_3 in CH_4/CO_2 reforming at 700 °C recorded at (a) 0 h, (b) 4 h, (c) 8 h, (d) 12 h and (e) 16 h on-stream time.

(Fig. 9) is an indication of the occurrence of RWGS reaction. With prolong on-stream time, the generation of carbon nanotubes and/or amorphous carbon (Fig. 10(i) and (iii)) would enhance the presence of hydrogen atoms, a condition that favors the RWGS reaction.

The HRTEM images observed over La_2NiO_4 and 10%NiO/CeO_2–La_2O_3 after CH_4/CO_2 reforming indicated two kinds of carbon species. On La_2NiO_4, there was copious amount of rope-like nanotubes with outer diameter ranging from 15 nm to 60 nm and with tips capped by Ni particles (Fig. 10(i)); such a kind of high Ni dispersion could contribute to the enhanced catalytic activity of La_2NiO_4. On 10%NiO/CeO_2–La_2O_3, a corrugated sheet-like carbon deposition was observed (Fig. 10(ii)), and at high magnification one can even detect the existence of graphitic structure (Fig. 10(iii)). According to the results of EDX analysis, approximately 65% of the detected carbon was deposited on 10%NiO/CeO_2–La_2O_3 during the

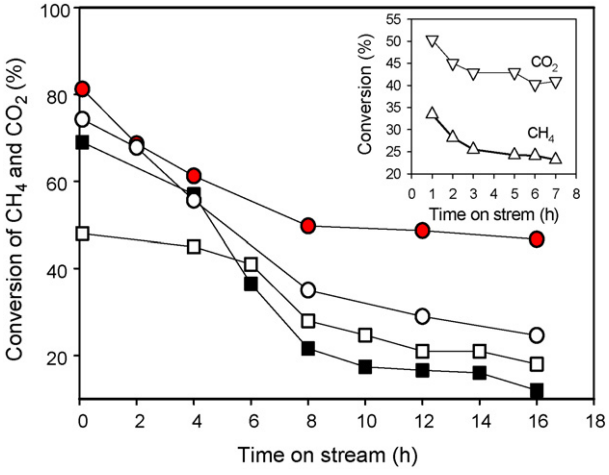

Fig. 9. Conversion of CH_4 (■) and CO_2 (●) over La_2NiO_4 and conversion of CH_4 (□) and CO_2 (○) over 10%NiO/CeO_2–La_2O_3, estimated based on peak areas (inset is the conversion of CH_4 and CO_2 observed over 10%NiO/CeO_2–La_2O_3 on a conventional reactor under the same condition).

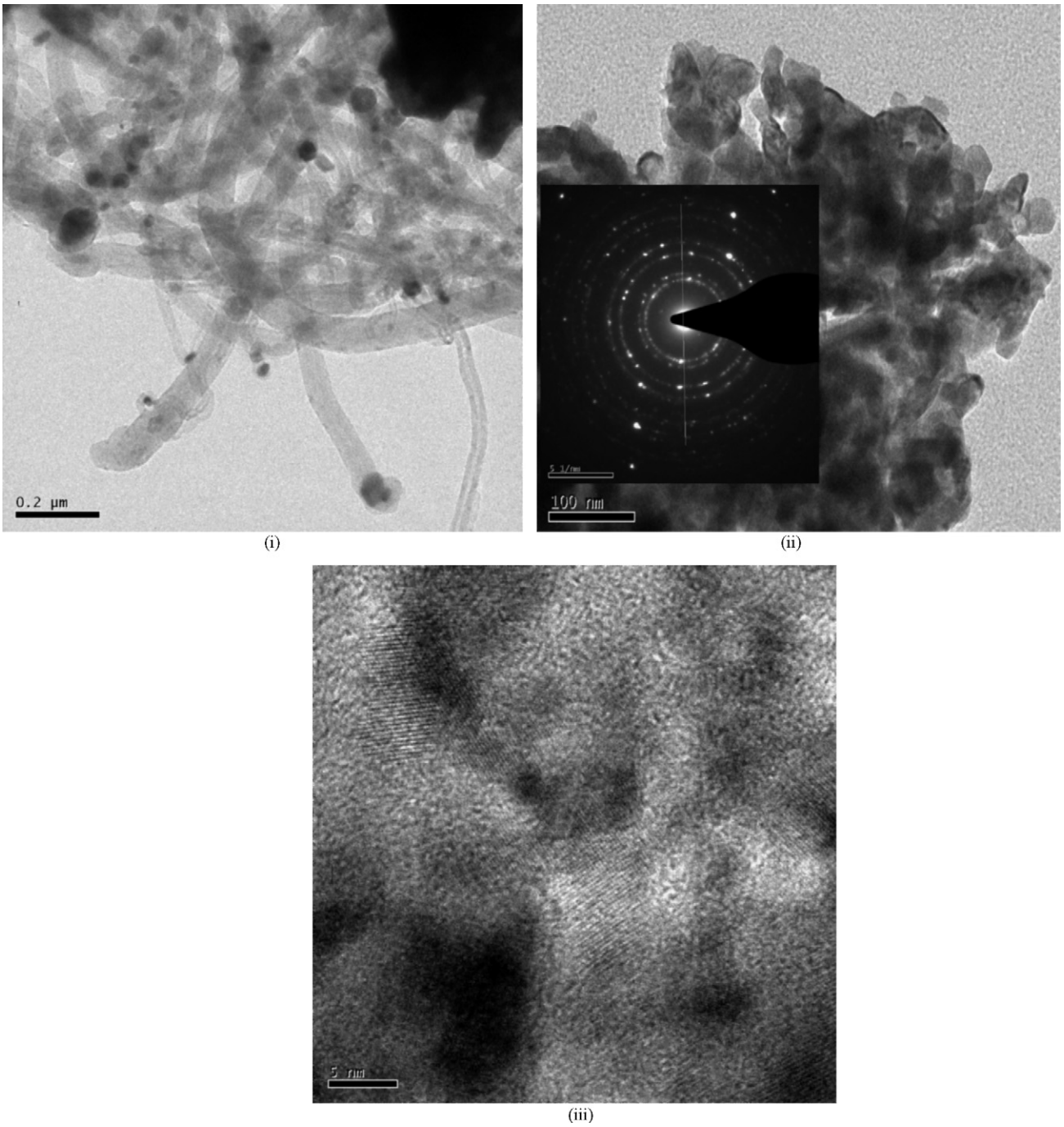

(i) (ii) (iii)

Fig. 10. HRTEM images of carbon deposition on (i) La_2NiO_4 and (ii and iii) on 10%NiO/CeO_2–La_2O_3; inset of (ii) is SAED pattern of 10%NiO/CeO_2–La_2O_3.

reforming reaction. The spotty rings in SAED pattern (inset of Fig. 10(ii)) implied that there were metal particles of relatively large size, suggesting that there was aggregation of Ni particles during the reaction.

4. Conclusion

In TOF-MS studies, the CH_x and OH intermediates were detected over the 10%NiO/CeO_2–La_2O_3 catalyst in CH_4/CO_2 reforming as well as in direct CH_4 decomposition under the condition of supersonic jet expansion. The species detected by the TOF-MS technique was related to a multi-photon ionization of CH_4, CO_2 and H_2O excited by an Nd:YAG laser (266 nm). The detection of H_2O signal in CRDS studies during CH_4/CO_2 reforming further confirmed the occurrence of the RWGS reaction. By means of the CRDS technique, we investigated the influence of reaction conditions such as temperature and on-stream time on the RWGS reaction, a reaction considered to be difficult to analyze due to the poor detection of H_2O in conventional chromatographic methods. The outcomes of TEM and TPR analysis and the results of CO_2 conversion verified that La_2NiO_4 was significantly superior to 10%NiO/CeO_2–La_2O_3.

At the later stage of the reaction, the slightly higher CH_4 conversion over 10%NiO/CeO_2–La_2O_3 is attributed to the acidic property and the oxygen storage ability of CeO_2 whereas the decline in CO_2 conversion over La_2NiO_4 related to the deterioration in basic property and spinal structure of La_2NiO_4.

Acknowledgement

The work described here was supported by a grant from the Research Grants Council of the Hong Kong Special Administrative Region, China (Project No. HKU 7101/02P).

References

[1] J.R.H. Ross, A.N.J. van Keulen, M.E.S. Hegarty, K. Seshan, Catal. Today 30 (1996) 193.
[2] S.B. Wang, G.Q. Lu, Energy Fuel 10 (1996) 896.
[3] Z.L. Zhang, X.E. Verykios, Appl. Catal. A 138 (1996) 109.
[4] A. Takano, T. Tagawa, S.J. Goto, J. Chem. Eng. Jpn. 27 (1994) 727.
[5] F. Solymosi, G. Kustan, A. Erdohelyi, Catal. Lett. 11 (1991) 149.
[6] Z.L. Zhang, V.A. Tsipouriari, A.M. Efstathiou, X.E. Verykios, J. Catal. 158 (1996) 51.
[7] W.D. Zhang, B.S. Liu, C. Zhu, Y.L. Tian, Appl. Catal. A 292 (2005) 138.
[8] B.S. Liu, J.Z. Gong, C.T. Au, Chin. J. Catal. 25 (2004) 15.
[9] B.S. Liu, L.Z. Gao, C.T. Au, Appl. Catal. A 235 (2002) 193–206.
[10] B.S. Liu, C.T. Au, Appl. Catal. A 244 (2003) 181.
[11] W.D. Zhang, B.S. Liu, Y.L. Tian, Catal. Commun. 8 (2007) 661.
[12] A. Valentini, N.L.V. Carrenõ, L.F.D. Probst, A. Barison, A.G. Ferreira, E.R. Leite, E. Longo, Appl. Catal. A 310 (2006) 174.
[13] H.-S. Roh, H.S. Potdar, K.-W. Jun, Catal. Today 93–95 (2004) 39.
[14] N.A. Echimuthu, K.K. Pant, S.C. Dhingra, R. Bhalla, Ind. Eng. Chem. Res. 45 (22) (2006) 7435.
[15] L. Romm, G.A. Somorjai, Catal. Lett. 64 (2000) 85.
[16] L. Romm, G.A. Somorjai, Top. Catal. 20 (2002) 53.
[17] B.S. Liu, J.W.H. Leung, L. Li, C.T. Au, A.S.-C. Cheung, Chem. Phys. Lett. 430 (2006) 210.
[18] S Busch, M.A. Busch (Eds.), Cavity ring-down spectroscopy—an ultra-trace absorption measurement technique, ACS Symp. Ser. 720, American Chemical Society, Washington, DC, 1999.
[19] B.S. Liu, C.T. Au, Catal. Lett. 85 (3–4) (2003) 165.
[20] T.M. Ma, J.W.H. Leung, A.S.-C. Cheung, Chem. Phys. Lett. 385 (2004) 259.
[21] T.M. Ma, J.W.H. Leung, A.S.-C. Cheung, J. Phys. Chem. A 108 (2004) 5333.
[22] B.S. Liu, L. Li, C.T. Au, A.S.-C. Cheung, Catal. Lett. 108 (2006) 37.
[23] B.S. Liu, D.C. Tang, C.T. Au, Micropor. Mesopor. Mater. 86 (2005) 106.
[24] J.M. Hollas, High Resolution Spectroscopy, 2nd ed., John Wiley & Son, 1998.
[25] M. Hipper, M. Quack, J. Chem. Phys. 16 (2002) 6045.
[26] R.A. Toth, Appl. Opt. 33 (1994) 4851.
[27] C.E. Miller, L. Brown, J. Mol. Spectrosc. 228 (2004) 329.
[28] L.A. Rothman, et al. J. Quant. Spectrosc. Rad. Trans. 96 (2005) 193.
[29] A. McIlroy, Chem. Phys. Lett. 296 (1998) 151–158.
[30] S.B. Wang, G.Q. Lu, Appl. Catal. B 19 (1998) 267.